PERGAMON

Computers and Structures 68 (1998) 445–459

Computers & Structures

Determination of wire recovery length in steel cables and its practical applications

Mohammed Raoof[a], Ivana Kraincanic[b]

[a]Civil and Building Engineering Department, Loughborough University, Loughborough, Leicestershire, LE11 3TU, U.K.
[b]School of Construction, South Bank University, Wandsworth Road, London, SW8 2JZ, U.K.

Received 9 January 1997; received in revised form 5 February 1998

Abstract

In the presence of relatively significant states of radial pressures between the helical wires of a steel cable (spiral strand and/or wire rope), and significant levels of interwire friction, the individual broken wires tend to take up their appropriate share of the axial load within a certain length from the fractured end, which is called the recovery (or development) length.

The paper presents full details of the formulations for determining the magnitude of recovery length in any layer of an axially loaded multi-layered spiral strand with any construction details. The formulations are developed for cases of fully bedded-in (old) spiral strands within which the pattern of interlayer contact forces and associated significant values of line-contact normal forces between adjacent wires in any layer, are fully stabilised, and also for cases when (in the presence of gaps between adjacent wires) hoop line-contact forces do not exist and only radial forces are present.

Based on a previously reported extensive series of theoretical parametric studies using a wide range of spiral strand constructions with widely different wire (and cable) diameters and lay angles, a very simple method (aimed at practising engineers) for determining the magnitude of recovery length in any layer of an axially loaded spiral strand with any type of construction details is prestented.

Using the final outcome of theoretical parametric studies, the minimum length of test specimens for axial fatigue tests whose test data may safely be used for estimating the axial fatigue lives of the much longer cables under service conditions may now be determined in a straightforward fashion. Moreover, the control length over which one should count the number of broken wires for cable discard purposes is suggested to be equal to one recovery length whose upper bound value for both spiral strands and/or wire ropes with any construction details is theoretically shown to be equal to 2.5 lay lengths.

Keywords: Wire recovery length; Steel cables; Multi-layered spiral strand; Radial forces

1. Notation

A	$\pi D^2/4$, wire cross-section area
b	half-width of line-contact patch
D	wire diameter
d	strand outer diameter
E	Young's modulus for steel
$f_{i+1,i}$	magnitude of the radial contact force per unit length between the wires in layers i and $i+1$
$f_{i-1,i}$	magnitude of the radial contact force per unit length between the wires in layers i and $i-1$
j	$=i+1$
l_{fs}^{i}	recovery length in layer i
N	number of layers
N_{T}	total number of wires in a strand
n	number of wires in each layer, number of sub-divisions
p	pitch of the wire
P_{RC}	line-contact force for an assumed single layer strand with a rigid core
$P_{\mathrm{MS}i}$	line-contact force in layer i of a multi-layered spiral strand
$Q_1^{(j)}$, $Q_2^{(j)}$	assumed tensile forces at the ends of interval j
R	wire radius

0045-7949/98/$19.00
PII: S0045-7949(98)00088-1

r	$= r_i - D_i/2$
r_i	helix radius in layer i
S_1	wire axial strain
S'_1	strand axial strain
S'_{2C}	rigid body motion including contact patch effects
S_2	normal strain between wires in line-contact
T	wire tension
$T_i\,(x)$	magnitude of the tensile force in a fractured wire in layer i at a distance x
X_i	the body force per unit length in layer i
X_{Ri}	magnitude of the clench force provided by each layer i acting on layer $i+1$
X_{MSj}	total radial force experienced by layer $j = i+1$ in a multi-layered spiral strand
Δx	length of interval
x	spacing between the contact patches along the concave side of a helical wire
x'	spacing of contact points on the convex side of wires
α	lay angle
α'	lay angle after deformation
γ_i	helix angle in layer i $(= \pi/2 - \alpha_i)$
$\overline{\gamma}_i$, $\underline{\gamma}_i$	helix angles on the upper and lower lines of contact of a wire in layer i, respectively
δ_n	normal approach of distant points in the Hertz problem
μ	co-efficient of friction
υ	Poisson's ratio
ζ	co-ordinate along the fractured wire with the fractured end denoted by $\zeta = 0$

Superscript and subscript

i	layer number (outer layer: $i = 1$)
j	interval number

2. Introduction

There is currently a discernible trend towards the requirement of certifying authorities for operators to demonstrate, both at the design stage and during its lifetime, the structural integrity of offshore installations such as compliantly moored structures. This has led to the need for an adequate procedure for predicting the fatigue endurance of mooring components coupled with realistic discard criteria for large diameter steel cables (spiral strands and wire ropes) for which until fairly recently, there was little reliable and publicly available literature. Large diameter cables also form an important part of suspension and cable-stayed bridging applications, amongst others.

With the passage of time and when exposed to various detrimental effects such as fatigue loading and/or stress corrosion, the individual component wires may break. The wire breakages may be external and/or internal, and internal wire breakages are invariably difficult to detect reliably by currently available methods of inspection, although some encouraging progress has been made in fairly recent years.

In the presence of relatively significant states of radial pressure between the wires due to their helical nature in spiral strands and/or wire ropes, and significant levels of interwire friction, the individual broken wires tend to take up their appropriate share of the axial load within a certain length from the fractured end, which is called the recovery (or development) length.

A knowledge of recovery length should prove useful when developing discard criteria for cables based on the remaining fatigue life (or strength). Moreover, as discussed by Raoof and Hobbs [1] a knowledge of the recovery length enables one to determine the appropriate minimum length of test specimens to be used for axial fatigue tests in order for the fatigue results to represent the actual behaviour of the much longer cables under service conditions.

It is now well established that, depending on the type of cable construction and nature of application, the influence of broken wires on the strength of a cable is not directly equivalent to a loss of area of steel; the number and distribution of wire breaks around a cable cross section and also along its length are both important. This, in turn, depends on the type of cable construction and its state of internal lubrication. Formation of multiple breaks along any individual wire is a relatively common occurrence. The performance of a wire rope is usually not affected by an occasional broken wire in the cable. With sufficient friction, a broken wire will be capable of supporting its total share of the load in a relatively short length. Obviously, multiple wire breaks in a relatively short length of the cable may have a significant influence on the cable's load-carrying capacity. On the experimental side, several investigators have used methods of varying sophistication for measuring the recovery lengths of individual wires in axially loaded spiral strands and ropes [2–5]. The recovery length for the individual wires in a helical cable is usually given as a percentage of the lay length of the cable under investigation. It is shown that the recovery length is a function of the type of cable construction.

Chein and Costello [6] published an analytical model for estimating the recovery length in cables. They used the classical rigid-plastic Coulomb friction model, and invoked Saint-Venant's principle to investigate the recovery length of the central (straight) core wire in a simple seven-wire helical strand. Raoof [7] extended the theoretical model of Chein and Costello [6] to include the transition between the full-slip to no-slip friction interactions along the core (straight) wire of an axially preloaded and multi-layered helical strand.

Raoof's model was based on an extension of a previously reported orthotropic sheet theory [8] and well-established results in the field of contact between rough and elastic bodies [9]. Later work by Raoof and Huang [10] addressed the problem of estimating the recovery length in parallel wire cables prestressed by external wrapping or intermittent bands (used as, for example, the main cables in suspension bridges). In their work, Raoof and Huang [10] spotted an oversight in Gjelsvik's [11] model on the same problem, and extended Gjelsvik's model to cater for the interwire no-slip to full-slip transition along the recovery length.

Recently, the present authors reported [12] the salient features of a theoretical model for determining the recovery length in the helical wires in any internal layer of an axially preloaded multi-layered spiral strand with the effect of hoop and radial interwire contact forces fully accounted for. Indeed, using theoretical parametric studies which covered the full practical range of cable (and wire) diameters and lay angles, a straightforward approach for determining the recovery length was suggested, which may be particularly useful for practising engineers. However, due to space limitations, only *part* of the theoretical formulations were reported, and *no* methods of solution for the complex final equation defining the magnitude of recovery length, were given. Instead, much attention was devoted to the presentation of the final numerical results and a discussion of their practical implications. Final numerical results relating to *sheathed* spiral strands in deep water platform applications have also been presented in another publication by the present authors [13].

The purpose of this paper is to present full details of the formulations used for arriving at the already reported numerical results with particular emphasis on the method(s) of solution for the complex final equation defining the value of recovery length based on estimates of interwire hoop and radial forces as predicted by the orthotropic sheet concept. As a double check, Leclair's [14] method (as opposed to the orthotropic sheet concept) will also be fully utilised for estimating interwire contact forces and developing the formulations for estimating the magnitude of recovery length in the absence of hoop contact forces. Moreover, using the final numerical results, recommendations will be made for a very simple means of determining the *control length* for any type of spiral strand (or indeed wire rope) construction aimed at practising engineers. The control length being defined as the appropriate length of the cable along which one should count the number of broken wires for cable discard purposes as recommended by various codes of practice. As a pre-requisite to this, however, full details of the theoretical formulations will be presented next.

3. Theory

3.1. Determination of the normal contact forces in an intact spiral strand

Full details of the derivations are given elsewhere [8] and only the final formulations will be presented in the following. As demonstrated in the next section, the various parameters mentioned in the following play a central role in developing the model for determining the recovery length.

Very briefly, in the theoretical orthotropic sheet model each layer of wires in a multi-layered helical strand is treated as a statically indeterminate orthotropic cylinder with a complaint core. The core resists the 'rigid body' radial movements, which would occur in its absence because of the change of lay angle from α to α' as the axial load changes and the wires assume a closer packing. Taking a single layer of wires with a core for a given cable axial strain, S'_1, the core is initially removed and the rigid body motion, S'_{2c}, including contact patch effects, is calculated. Replacing the core, and enforcing compatibility of radial movements, the deformations in the hoop direction and the line contact forces may then be computed as functions of the net radial strain, S'_2, which is the one used for the orthotropic sheet. Using such a technique, the magnitude of the line-contact force, P_{RCi}, for an assumed single layer helical strand with a rigid core whose single outer layer corresponds to the layer i in a multi-layered strand whose outer layer is denoted by $i = 1$, is found by solving the following:

$$\delta_{ni} = \frac{4P_{RCi}(1-\nu^2)}{\pi E}\left[\frac{1}{3} + 1n\frac{D_i}{b_i}\right], \tag{1a}$$

where, the widths of the line-contact patches in layer i, $2b_i$, with wire diameters, D_i, whose Young's modulus and Poisson's ratio are E and ν, respectively, are given by

$$2b_i = 1.6\left[\frac{P_{RCi}D_i(1-\nu^2)}{E}\right]^{\frac{1}{2}}. \tag{1b}$$

In Eq. (1a), the approach distance between centres of adjacent wires in line- contact, δ_{ni}, under normal strain, S_{2i}, is given by

$$\delta_{ni} = S_{2i}D_i, \tag{2}$$

where, for a given lay angle in layer i, α_i, and strand axial strain S'_1, S_{2i} may be calculated from Eqs. (2)–(8) in ref (8): S_{2i} denotes the normal strain between the centres of wires in line-contact in layer i for the case of an assumed single layer strand with a rigid core whose helical wires have helix radius r_i, with a total number of n_i wires in the layer.

The magnitude of radial force, X_{RCi}, in the single layer strand with a rigid core, on the other hand, is (based on hoop tension formula)

$$X_{RCi} = \frac{T_i \sin^2 \alpha_i}{r_i}, \tag{3}$$

where, the axial tension in helical wires of layer i, $T_i = EA_iS_1^i$; with each wire in layer i having normal cross-section area $A_i = \pi D_i^2/4$. The magnitude of the wire axial strain in layer i is denoted by S_1^i, and may be obtained from the following [15]:

$$\frac{S_1^i}{S_1'} = 1 - 0.00255\alpha_i + 0.000215\alpha_i^2 - 0.0000271\alpha_i^3, \tag{4}$$

where, S_1' = strand axial strain which (for a given cable axial load) may easily be calculated once the value of strand effective Young's modulus is known. Note that α_i in Eq. (4) relates to the absolute magnitude of lay angle (irrespective of lay direction) in layer i and is expressed in degrees.

The magnitude of the helix radius in layer i, r_i, is [16]

$$r_i = R_i \left[1 + \frac{\tan^2\left(\frac{\pi}{2} - \frac{\pi}{n_i}\right)}{\cos^2 \alpha_i} \right]^{\frac{1}{2}}, \tag{5}$$

where R_i = wire radius in layer i whose number of wires and lay angle are denoted by n_i and α_i, respectively.

The magnitude of the clench force, X_{Ri}, as shown in Fig. 1, provided (under a spiral strand axial strain, S_1') by each layer i acting on layer $i + 1$ is given by

$$X_{Ri} = X_{MSi} - 2P_{MSi} \cos \beta_i, \tag{6}$$

where, the angle β_i in Fig. 1 is given by [17]

$$\cos \beta_i = \frac{1}{\sin^2 \alpha_i} \left\{ \sqrt{1 + \frac{\tan^2\left(\frac{\pi}{2} - \frac{\pi}{n_i}\right)}{\cos^2 \alpha_i}} - \sqrt{\tan^2\left(\frac{\pi}{2} - \frac{\pi}{n_i}\right)\left[1 + \frac{1}{\cot^2 \alpha_i \cos^2\left(\frac{\pi}{2} - \frac{\pi}{n_i}\right)\left[\cos^2 \alpha_i + \tan^2\left(\frac{\pi}{2} - \frac{\pi}{n_i}\right)\right]}\right]} + \cos^4 \alpha_i \right\}. \tag{7}$$

Note that Eq. (6) is the correct version of Eq. (19) in ref (8). All the results based on the orthotropic sheet theory reported to date employ Eq. (6) in the above.

Each wire in layer $j = i + 1$ thus experiences a total radial force, X_{MSj}, given by

$$X_{MSj} = EA_j \frac{S_1^i \sin^2 \alpha_j}{r_j} + X_{Ri} \frac{x_i}{x_j'}, \tag{8}$$

where, the spacings between the contact patches along the concave side of a wire in layer i,x_i, with n_j wires in layer $j = i + 1$, are [18]

$$x_i = \frac{2\pi r}{n_j} \frac{\cos \alpha_j}{\sin(\alpha_i - \alpha_j)} \tag{9}$$

and the spacings of contact patches on the convex side of a helical wire in layer j, x_j', with n_i wires in layer $i = j - 1$ is given by

$$x_j' = \frac{2\pi r}{n_i} \frac{\cos \alpha_i}{\sin(\alpha_i - \alpha_j)} \tag{10}$$

with

$$r = r_i - \frac{D_i}{2}. \tag{11}$$

Using Eqs. (1)–(5), estimates of P_{RCi} and X_{RCi} are obtained for a number of S_1' values for all the layers i in the strand in order to produce P_{RCi} against X_{RCi} plots for various layers. Calculation of the normal (hoop and radial) forces in the multi-layered assembly (P_{MCi} and X_{MSi}) then follows.

For the outer layer (layer number 1) the hoop forces are a function of the clench (radial) force generated in the helical wires so that P_{RC1}/X_{RC1} and P_{MS1}/X_{MS1} relationships are identical. For the other (inner) layers, the additional clench force provided by the outer layer i on layer $i + 1$, X_{R_i}, is given by Eq. (6): using the previously calculated P_{RCj}/X_{RCj} data it is then possible to find corresponding values for P_{MSj} and X_{MSj} for layer $j = i + 1$. The process is then repeated, moving in another layer [19].

3.2. Calculation of the recovery length

The tension in a fractured wire in layer i, T_i (ζ), increases from zero at the fractured end to T_i ($\zeta = l_{fs}$) = $EA_iS_1^i$ at the end of the recovery length where the wire axial tension becomes equal to that of the neighbouring unfractured wires in the same layer, with l_{fs} = recovery length, A_i = wire normal cross-section area in layer i whose axial strain is S_1^i and E is the Young's modulus for steel. The gradual increase in tension is partly due to the radial forces exerted on the fractured wire from the inner and outer neighbouring layers $i-1$ and $i + 1$, and partly due to the hoop forces exerted on the fractured wire from the unfractured wires in the same layer i which touch the wire under consideration in line-contact, Fig. 1. Using the principle of axial equilibrium one gets

$$T_i(x) = \int_0^x \mu \left[X_{R,i-1} \frac{x_{i-1}}{x_i'} + 2P_{MSi}(\zeta) + X_{Ri}(\zeta) \right] d\zeta. \tag{12}$$

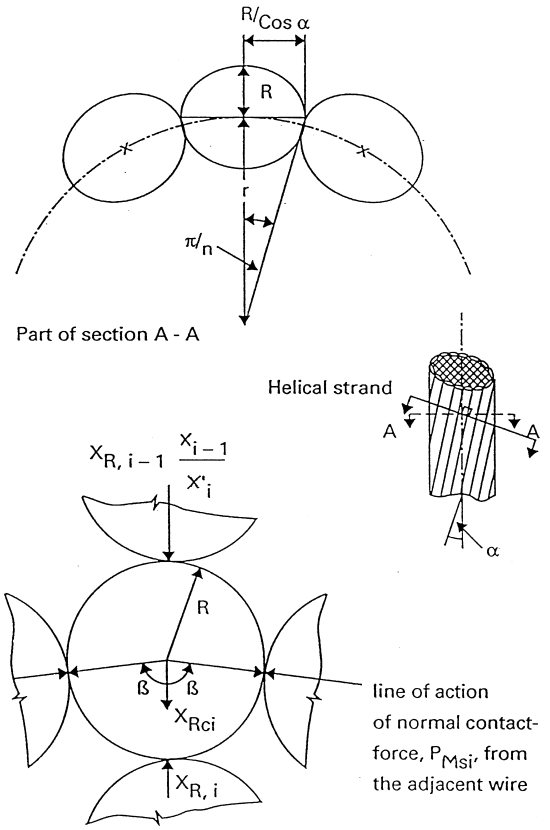

Fig. 1. Pattern of interwire/interlayer contact forces in an axially loaded spiral strand.

Using Eqs. (6) and (12)

$$T_i(x) = \mu X_{R,i-1}\frac{x_{i-1}}{x'_i}x + 2\mu\int_0^x P_{MSi}(\zeta)\mathrm{d}\zeta + \mu\int_0^x [X_{MSi}(\zeta) - 2P_{MSi}(\zeta)\cos\beta_i]\mathrm{d}\zeta. \quad (13)$$

Eqs. (3), (8) and (13) may then be used to arrive at the following

$$T_i(x) = 2\mu X_{R,i-1}\frac{x_{i-1}}{x'_i}x + \mu\frac{\sin^2\alpha_i}{r_i}\int_0^x T_i(\zeta)\mathrm{d}\zeta + 2\mu(1-\cos\beta_i)\int_0^x P_{MSi}(\zeta)\mathrm{d}\zeta. \quad (14)$$

Assuming that for a large diameter spiral strand, fracture of an individual helical wire (i.e. loss of its axial force) does not significantly alter the axial forces in the other (unfractured) helical wires, the relationship between P_{MSi} and X_{MSi} is (as discussed in the previous section) already known. In addition, using Eqs. (3) and (8)

$$X_{MSi}(\zeta) = \frac{\sin^2\alpha_i}{r_i}T_i(\zeta) + X_{R,i-1}\frac{x_{i-1}}{x'_i} \quad (15)$$

therefore, at $\zeta = 0$,

$$X_{MSi}(0) = X_{R,i-1}\frac{x_{i-1}}{x'_i} \quad (16)$$

and, following Eqs. (14)–(16)

$$T_i(x) = 2\mu X_{R,i-1}\frac{x_{i-1}}{x'_i}x + \mu\frac{\sin^2\alpha_i}{r_i}\int_0^x T_i(\zeta)\mathrm{d}\zeta + 2\mu(1-\cos\beta_i)\frac{r_i}{\sin^2\alpha_i}\int_{X_{R,i-1}\frac{x_{i-1}}{x'_i}}^{\frac{\sin^2\alpha_i}{r_i}T_i(x)+X_{R,i-1}\frac{x_{i-1}}{x'_i}} \frac{P_{MSi}(X_{MSi})}{\frac{\mathrm{d}T_i(\zeta)}{\mathrm{d}\zeta}}\mathrm{d}X_{MSi}, \quad (17)$$

while, using Eq. (15)

$$\frac{\mathrm{d}X_{MSi}(\zeta)}{\mathrm{d}\zeta} = \frac{\sin^2\alpha_i}{r_i}\frac{\mathrm{d}T_i(\zeta)}{\mathrm{d}\zeta} \quad (18)$$

with all the other parameters known, Eq. (17) provides the value of recovery length, l_{fs}, using the following numerical technique.

3.3. Method (a) of solution: non-linear

Sub-divide the pitch into n segments of length Δx with an assumed linear variation of $T(x)$ in the interval. In each interval, j, then, the following holds

$$\left[\frac{\mathrm{d}T(\zeta)}{\mathrm{d}\zeta}\right] \approx \frac{Q_2^{(j)} - Q_1^{(j)}}{\Delta x} \quad (19a)$$

$$= G_T \quad (19b)$$

where, $Q_1^{(j)}$ and $Q_2^{(j)}$ are the *assumed* tensile forces at the ends of interval j; with

$$\int_{x_{j-1}}^{x_j} T(\zeta)\mathrm{d}\zeta \approx \frac{1}{2}(Q_1^{(j)} + Q_2^{(j)})\Delta x \quad (20a)$$

$$= R_1 \quad (20b)$$

and

$$\int_{\frac{\sin^2\alpha_i}{r_i}T_{j-1}+X_{R,i-1}\frac{x_{i-1}}{x'_i}}^{\frac{\sin^2\alpha_i}{r_i}T_j+X_{R,i-1}\frac{x_{i-1}}{x'_i}} \frac{P_{MS}(X_{MS})}{G_T}\mathrm{d}X_{MS} = \frac{1}{G_T}\int_{\frac{\sin^2\alpha_i}{r_i}Q_1^{(j)}+X_{R,i-1}\frac{x_{i-1}}{x'_i}}^{\frac{\sin^2\alpha_i}{r_i}Q_2^{(j)}+X_{R,i-1}\frac{x_{i-1}}{x'_i}} P_{MS}(X_{MS})\mathrm{d}X_{MS} = R_2 \quad (21)$$

where, G_T is independent of X_{MS}.

For any interval j, Eq. (17) may then be written as

$$T_j = T_{j-1} + 2\mu X_{R,i-1}\frac{x_{i-1}}{x'_i}\Delta x + \mu\frac{\sin^2\alpha_i}{r_i}R_1 + 2\mu(1-\cos\beta_i)\frac{r_i}{\sin^2\alpha_i}R_2, \quad (22a)$$

where

$$T_{j-1} = Q_1^{(j)}. \quad (22b)$$

For the first interval (i.e. $j = 1$), the following may initially be assumed:

$$x_0 = 0 \quad (23a)$$

$$Q_1^{(1)} = 0 \quad (23b)$$

and

$$x_1 = \frac{\text{Pitch}}{n} = \Delta x \quad (23c)$$

$$Q_2^{(1)} = 2\mu X_{R,i-1}\frac{x_{i-1}}{x'_i}\Delta x, \quad (23d)$$

where, n = assumed number of sub-divisions.

Using (23a–d), find G_T, R_1 and R_2 from Eqs. (19)–(21), respectively. From Eq. (22), then, we have the new value of T_1 which will, in turn, by setting $Q_2^{(1)} = T_1$, be used for obtaining updated values for G_T, R_1 and R_2. The iteration process is repeated for a number of times until the calculated values of T_1 and $Q_2^{(1)}$ in the last iteration are sufficiently close.

In the second interval (i.e. $j = 2$), the following initial values of $Q_1^{(2)}$ and $Q_2^{(2)}$ may be assumed:

$$Q_1^{(2)} = Q_2^{(1)} \quad (23e)$$

and

$$Q_2^{(2)} = Q_1^{(2)} + G_T^{(1)}\Delta x. \quad (23f)$$

Eq. (23), thus, may be used in the iterative process as for T_1 to find the value of T_2 in the second interval, and so on.

The whole process is repeated until in some interval j, the magnitude of T_j is found to be greater than the corresponding tension in an unbroken wire. Wire recovery length in layer i, l_{fs}^i, is, then, given as

$$l_{fs}^i = j\Delta x. \quad (24)$$

Number of sub-divisions, n, is subsequently changed (by, say, a factor 2), and the process is repeated so that an alternative value of recovery length is found. The iteration is stopped when two sufficiently close estimates of recovery length are found.

It should be noted that as (in the presence of inter-wire friction in the hoop and radial directions) the axial force in the fractured wire increases in magnitude along the length of the wire from the fractured end, there exists some degree of non-linearity in the imposed levels of frictional forces on the fractured wire (such as those due to P_{MSi} and, hence, $X_{R,i}$). However, it may intuitively be assumed that the degree of non-linearity is not of much practical significance. In other words, it may be suggested that variation of the tension in the fractured wire along its length from the fractured end, x, is linear: this assumption, then, will considerably simplify the solution procedure for Eq. (17). This alternative (i.e. linearized) solution procedure will be referred to as method (b). Indeed, the simpler linear solution has been found to lead to reasonable predictions of recovery length. This simpler (alternative) method is particularly reasonable because the magnitude of the coefficient of friction between the heavily lubricated wires (which is a controlling parameter in the theoretical model) remains very unpredictable although one may reasonably assume its value to lie within certain bounds. Indeed, it may be argued that the coefficient of friction for even a given contact patch may vary during the working life of the cable and there are variations of the coefficient of friction over different contact patches throughout the internal structure of a spiral strand. Bearing this in mind, there is little point in trying to obtain mathematically exact estimates of recovery length, and, in view of the fact that the deviations from non-linearity have been found not be very significant, a linear solution would suffice for most practical situations.

3.4. Method (b) of solution: linear

The last two parts in Eq. (17) are functions of tension in the fractured wire, which will be assumed to be a linear function of the distance from the broken end, i.e.

$$T_i(x) = qx. \quad (25)$$

In the above, q is a constant and x is the distance from the fractured end. After substituting Eq. (25) into Eq. (17), the following expression is obtained, which may be solved using numerical techniques.

$$T_i(x) = 2\mu X_{R,i-1}\frac{x_{i-1}}{x'_i}x + \mu\frac{\sin^2\alpha_i}{r_i}q\frac{x^2}{2} + 2\mu(1-\cos\beta_i) \cdot \frac{r_i}{\sin^2\alpha_i}\frac{1}{q}\int_{X_{R,i-1}\frac{x_{i-1}}{x'_i}}^{\frac{\sin^2\alpha_i}{r_i}qx+X_{R,i-1}\frac{x_{i-1}}{x'_i}} P_{MSi}(X_{MSi})\,dX_{MSi}. \quad (26)$$

A value of x is initially assumed and noting that

$$T_i(x) = EA_i S_1^i \tag{27}$$

one may combine Eqs. (25) and (27) to find the value of q. After substituting Eq. (27) and the so-obtained value of q into Eq. (26), the solution may easily be found using, for example, the false position method [20]. This solution, then, gives the magnitude of the recovery length in layer i of an axially preloaded multi-layered spiral strand.

It should be pointed out that the values of circumferential (i.e. normal) contact forces as calculated by the orthotropic sheet theory only apply to fully bedded-in (i.e. old) strands with no gaps present between the wires in line-contact in various layers. As discussed at some length elsewhere [22], although for newly manufactured (but prestretched) strands, gaps may exist between the adjacent wires in a given layer, with the passage of time under working conditions, due to the occurrence of interwire fretting and bedding-in, these gaps gradually close-up and various adjacent wires in a given layer assume a state of full line-contact across which normal (hoop) contact forces are transmitted: this situation, however, has been shown by carefully conducted experiments [22] to take a rather long time, and during this period there will always be uncertainties regarding the exact magnitudes of line-contact forces between wires which is another crucial parameter as regards the presently reported formulations. Nevertheless, two extreme cases of zero or full-contact may be assumed where the full-contact hoop forces may be estimated by the previously presented formulations and the zero contact case will be discussed next.

3.5. Calculation of recovery length using Leclair's approach

Leclair [14], has presented a method for obtaining the magnitudes of radial contact forces in multi-layered spiral strands in the absence of any interwire contact forces in the hoop direction, where small gaps have been assumed to exist between the neighbouring wires in any given layer. As discussed later, the orthotropic sheet theory can (as an extreme case) also handle the zero line-contact force regime.

Using Leclair's method for obtaining the magnitude of radial forces, the magnitude of the tensile force in a fractured wire in layer i at a distance x from the broken end, $T_i(x)$, is

$$T_i(x) = \mu \int_0^x [f_{i+1,i} + X_i(\zeta) + f_{i-1,i}(\zeta)]\mathrm{d}\zeta, \tag{28}$$

where $f_{i+1,i}$ is the magnitude of radial contact force per until length between the wires in layers i and $i+1$ (which for a given strand axial load, is a constant)), $f_{i,i-1}$ is the radial contact force acting on the wire from the layer below which depends on the tension in the fractured wire, and X_i is the body force per unit length in layer i, i.e.

$$X_i(\zeta) = \frac{\cos^2 \gamma_i}{r_i} T_i(\zeta) \tag{29a}$$

$$= C_i T_i(\zeta). \tag{29b}$$

In the above, C_i is a constant, and γ_i represents the helix angle in layer i (i.e. $\gamma_i = \pi/2 - \alpha_i$) with r_i denoting the helix radius.

Re-stating Eq. (38) in ref. [14] (in the present notation)

$$f_{i-1,i}(\zeta) = X_i(\zeta) + \sum_{j=i+1}^{n} \frac{n_j p_i \cos \bar{\gamma}_i}{n_i p_j \cos \underline{\gamma}_i} \left(\prod_{k=i+1}^{j-1} \frac{\cos \bar{\gamma}_k}{\cos \underline{\gamma}_k} \right) X_j, \tag{30}$$

where, n_i and n_j are the number of wires (with p_i and p_j denoting their associated pitches) in layers i and j, respectively, with $\underline{\gamma}_i$ and $\bar{\gamma}_i$ defining the helix angles on the lower and upper lines of contact of a wire in layer i, respectively.

Eq. (30) may be rewritten as

$$f_{i-1,i}(\zeta) = X_i(\zeta) + B_i, \tag{31}$$

where B_i is a constant independent of distance along the wire. Using Eqs. (28), (29) and (31) the equivalent version of Eq. (22) (which is based on the orthotropic sheet concept) is given as

$$T_j = T_{j-1} + \mu A_{i+1} \Delta x + 2\mu C_i \int_{x_{j-1}}^{x_j} T(\zeta)\mathrm{d}(\zeta) + \mu B_i \Delta x, \tag{32}$$

where

$$A_{i+1} = f_{i+1,i} = \text{constant} \tag{33}$$

or

$$T_j = T_{j-1} + \mu(A_{i+1} + B_i)\Delta x + 2\mu C_i R_1. \tag{34}$$

In Eq. (34), R_1 is as defined in the previous section, i.e.

$$R_1 = \frac{Q_1^{(j)} + Q_2^{(j)}}{2} \Delta x, \tag{35}$$

where $Q_1^{(j)}$ and $Q_2^{(j)}$ are the *assumed* tensile forces at the ends of interval j. The solution technique then follows exactly the same route as that adopted for solving Eq. (22), with the proviso that in the iteration process for the first interval, it is assumed that

$$Q_1^{(1)} = 0 \tag{36}$$

$$Q_2^{(1)} = \mu(A_{i+1} + B_i)\Delta x. \tag{37}$$

In the same way as in the previous section, if one decides to use a linearized solution procedure, the tension in the fractured wire may be assumed to increase linearly along the broken wire, i.e. Eq. (25) may be assumed to hold. Under such conditions Eq. (28) may be written as

$$T_i(x) = \mu \int_0^x [f_{i+1,i} + C_i q\zeta + B_i]\mathrm{d}\zeta \tag{38}$$

and in Eq. (38)

$$x = \frac{T_i}{\mu(f_{i+1,i} + B_i + \frac{1}{2}C_i T_i)}, \tag{39}$$

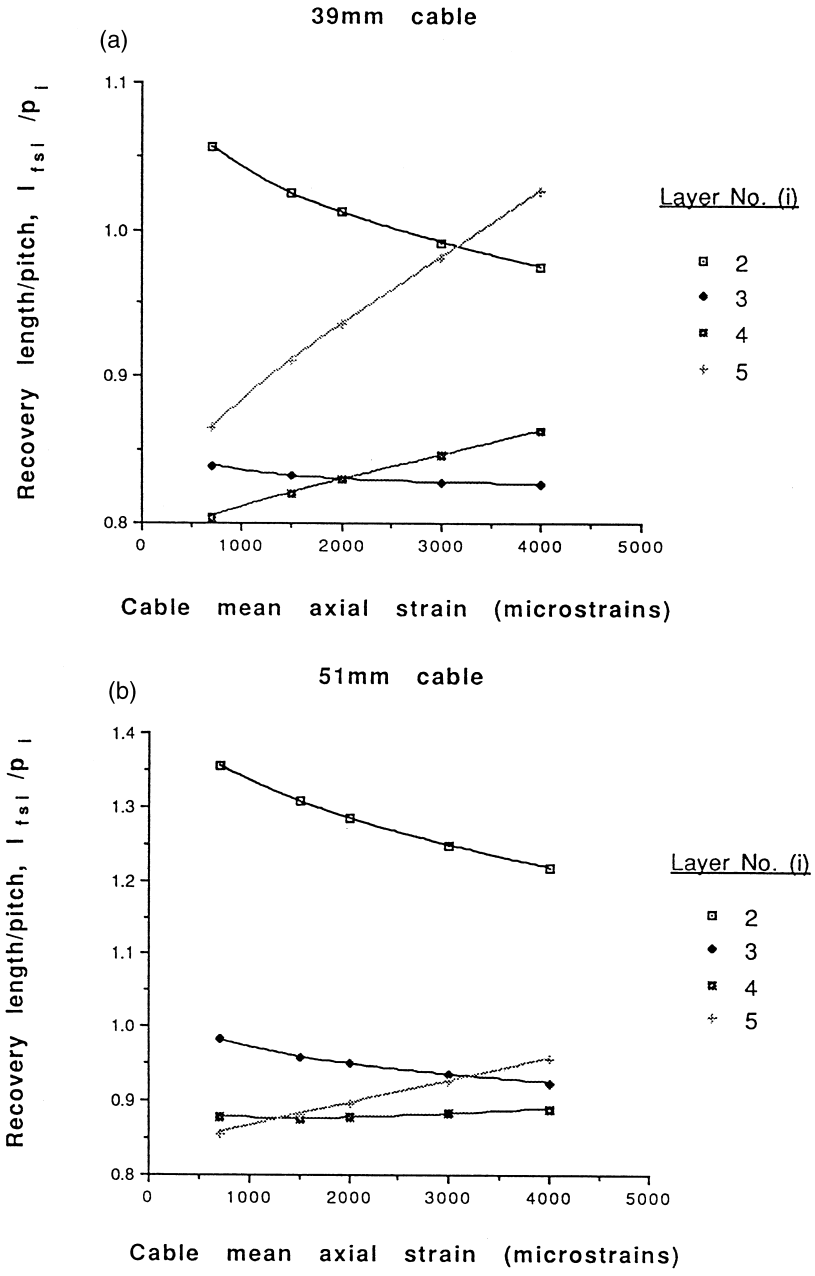

Fig. 2(a and b).

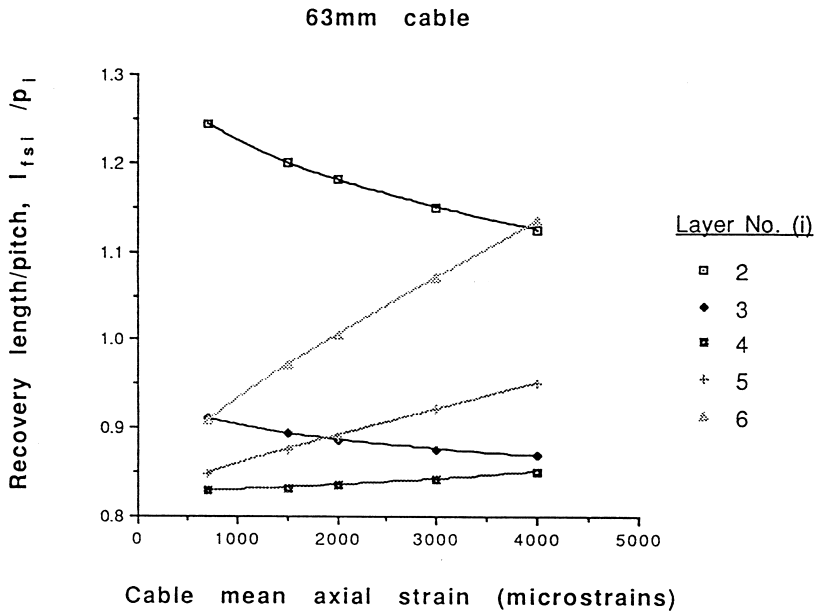

Fig. 2. Variations of recovery length vs cable mean axial strain, for various layers of different spiral strand constructions: (a) 39 mm O.D. strand; (b) 51 mm O.D. strand; (c) 63 mm O.D. strand.

where, x is the distance along the fractured wire from the broken end in which the wire achieves its full share of the tensile force.

4. Results and Discussion

Fig. 2(a–c) presents the estimates of recovery length in all the layers (except for the outer layer) of 39, 51 and 63 mm diameter spiral strands, respectively, as a function of the mean axial strain acting on the strands. The construction details for all these spiral strands are given elsewhere [12]), and a value of interwire coefficient of friction $\mu = 0.12$ is assumed for all the heavily lubricated galvanised wires [21]. Note that the recovery length in various layers is non-dimensionalised by dividing it by the lay length (pitch) of the helical wires in the same layer. The plots suggest that, depending on the location of the wire inside the strand, the magnitude of non-dimensionalised recovery length may either increase or decrease with increasing levels of strand mean axial strain. However, the variations are found to amount to no more than 10–20% of the mean value, over a wide range of cable mean axial strains, and in view of other uncertainties as regards, for example, the assumed constant value of the interwire coefficient of friction throughout the cable, and the exact patterns of interwire normal contact forces throughout the strands etc., such variations in the values of the recovery length are not believed to be of much practical significance.

The plots in Fig. 2(a–c) are all based on the non-linear method of solution [i.e. method (a)] for Eq. (17), with the magnitudes of normal hoop and radial interwire contact forces based on the estimates of the orthotropic sheet concept as presented earlier on in this paper. It should also be pointed out that numerical results for the magnitudes of recovery length for the same layers of 39, 51 and 63 mm diameter strands were also obtained using the simpler linear technique [i.e. method (b)], and the final results for both methods (a) and (b) were very similar: as previously discussed at some length [ref. to the paragraph following Eq. (24)], due to the ever present uncertainties associated with the estimated magnitudes of line-contact forces throughout a spiral strand and the assumed value of interwire coefficient of friction, the linearized solution should prove of sufficient accuracy for most practical applications (especially in view of the rather small degrees of non-linearities found). An account of the practical uses of the estimates of wire recovery length will be given in the next section which suggest that a rough (but simply obtained) estimate of wire recovery length is all that is needed in practical engineering applications. It has, however, been useful to carry out the fully non-linear analysis to verify that the degree of non-linearity is not significant and may safely be ignored in practice.

Using an extensive series of theoretical parametric studies [using method (a)] covering a wide range of spiral strand (and wire) diameters, lay angles, and strand mean axial strains within the working range

Table 1
Range of various strand parameters used in the study

Parameters	Range of parameters
Strand diameter, d (mm)	$16.4 \leq d \leq 184$
Number of layers, N	$2 \leq N \leq 11$
Number of wires in each layer, n	$12 \leq n \leq 74$
Total number of wires, N_T	$19 \leq N_T \leq 552$
Lay angle, α (degrees)	$11 \leq \alpha \leq 25$
Wire diameter, D (mm)	$2.36 \leq D \leq 6.55$

$0.0007 \leq S_1' \leq 0.004$, as fully reported elsewhere [12], (see Table 1) a generally applicable plot of wire recovery length/pitch in a layer versus lay angle in that layer for any layer of an axially preloaded spiral strand with any construction detail has been obtained and is presented in Fig. 3(b). In Fig. 3(b), which uses the same data points as in Fig. 3(a), a best-fit curve is included where (bearing in mind the previously discussed real life uncertainties regarding the assumed value of the coefficient of interwire friction and magnitude of line-contact forces) a reasonable correlation has been obtained between the individual data points and the fitted curve. Using this curve, then, it is possible to assess (with minimal effort) the magnitude of recovery length/pitch ratio for the wires in any layer of an axially loaded spiral strand, once the lay angle of wires in that layer are specified. It should at once be pointed out that traditionally the field of wire rope has been considered as an art and not an exact science, and it is an area where the rule of thumb reigns supreme. What cable manufactures and user require is not a mathematically complex and so-called exact solution, but a simple and reasonable means of estimating various structural characteristics of the cables. For these pur-

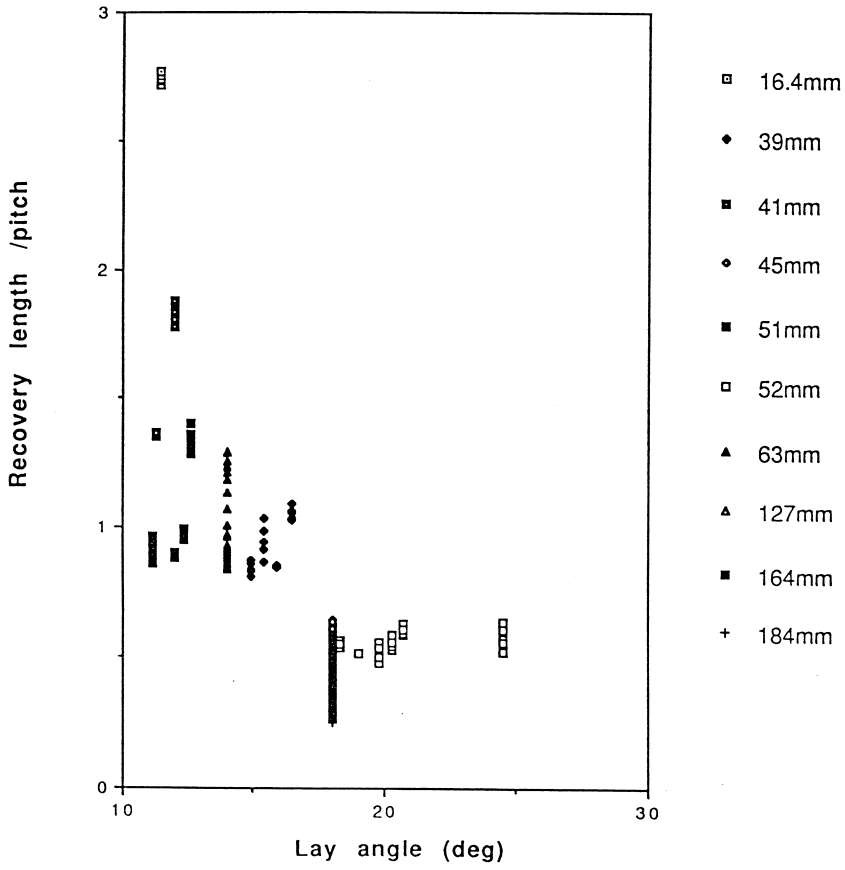

Fig. 3(a).

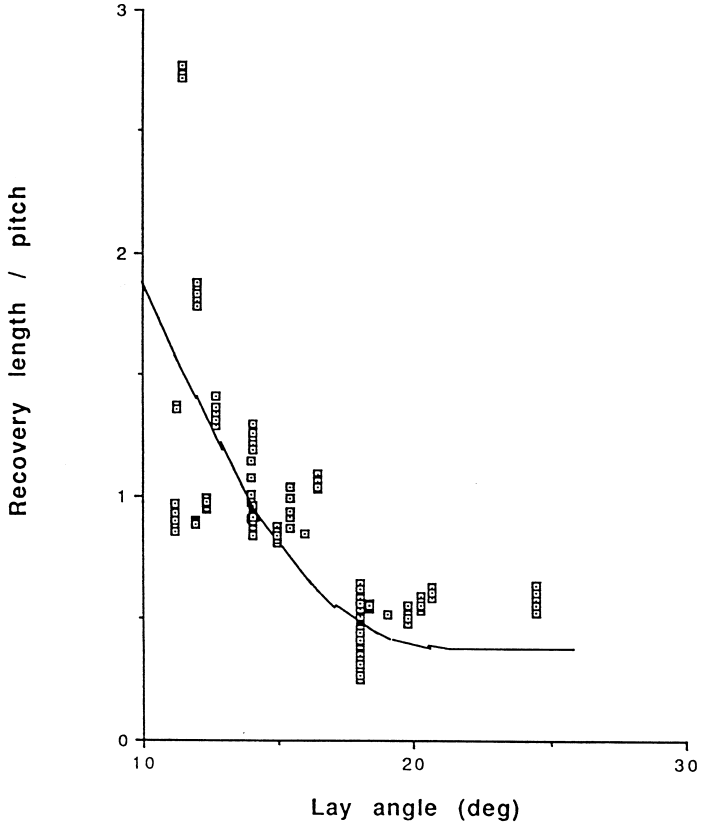

Fig. 3. Variations of recovery length with changes in the values of lay angle in various layers of a number of fully bedded-in spiral strand constructions: (a) detailed data points; (b) fitted curve to the theoretical data.

poses, therefore, easy to use (practical) recommendations are most welcomed by industry, and this is the underlying reason for producing the fitted curve in Fig. 3(b) which (as discussed in the next section) should suffice for practical purposes despite the fact that there are some (sometimes, apparently large) deviations of individual data points from the fitted line.

As fully discussed by Raoof [22], in newly manufactured spiral strands there may (in contrast to the underlying assumptions in the orthotropic sheet theory) exist partial or no line-contact normal forces between adjacent wires in a given layer. As a limiting case, one may then assume the line-contact forces between the wires in the same layer to vanish altogether and repeat the theoretical parametric studies for calculating the recovery lengths: the results for the recovery length corresponding to this case are presented in Fig. 4(a). The results plotted in this figure are found to suffer from more scatter than the data in Fig. 3 (which relates to the fully bedded-in strands), and the recovery length is found to increase slightly in the absence of line-contact forces. Nevertheless, in both cases the recovery length shows some tendency to decrease with increases in the magnitude of the lay angle. Finally as an alternative approach to the orthotropic sheet concept, the plots in Fig. 4(b) show similar trends of results, and these are obtained by Leclair's [14] method for the estimation of the radial normal contact forces, and use the solution method (a) for solving the complex equation for determining the magnitude of recovery length.

Although the fitted curve in Fig. 3(b) is, strictly speaking derived for enabling one to determine the magnitude of recovery length in any layer of a spiral strand, it also provides a simple means of estimating the upper bound to the value of recovery length of a broken wire in an axially loaded wire rope. This is the case, simply because due to the presence of additional compressive forces exerted by the neighbouring spiral strands in a wire rope, the magnitudes of the frictional forces acting on helical wires in any strand of a wire rope will (compared to that in an isolated strand) increase, hence, leading to a smaller value of recovery length than that predicted by the fitted curve in Fig. 3(b).

On the experimental side, several investigators have used various methods for measuring the recovery lengths of individual wires in axially loaded cables. Davidsson [2] concludes that for the outer wires of regular and Lang's lay six-strand ropes, the recovery length is between 1.3 and 2.0 of the rope lay and recommends an average value of 1.7 to be used in the absence of test data. Wiek [3], on the other hand, quotes 1.5–6 as the recovery length of six-strand ropes, dependent upon rope diameter, construction and type of lay. In his experiments on 53 mm, 6 × 35 Lang's lay rope, Hankus [4] found a recovery length of three times the rope length, which is rather different from the values of 1–1.5 quoted by Chaplin and Tantrum [5] who worked on 19 mm, 6 × 19 ordinary lay ropes. It is encouraging that the range of published test data from various sources are found to provide a similar range of values for recovery length as given by the theoretical data in Fig. 3(b) which suggests a range of, say, 0.5–2.5 for the ratio of recovery length/pitch.

Finally, as fully discussed by Raoof [7] and Raoof and Huang [10], in general, the recovery length will be divided into two no-slip and full-slip parts with the full-slip region being nearest to the fractured end. The present paper has addressed only the occurrence of full-slip (i.e. Coulomb friction) along the entire recovery length, because, following Raoof [7], numerical data has suggested that the no-slip portion of the recovery length is generally small compared with the full-slip portion, and (in view of other uncertainties surrounding the problem) the no-slip portion may reasonably be ignored.

5. Practical Applications

A knowledge of the magnitude of recovery length in steel cables (spiral strands and wire ropes) will enable one to determine the minimum length of test specimens for axial fatigue life prediction of the much longer cables under service conditions. As discussed in the introduction, an appropriate control length for steel cables over which the number of broken wires may be counted for cable discard purposes, may also be determined using the predicted values of recovery length.

The question of determining the minimum length of test specimens for axial fatigue conditions has been dealt with in some detail by Raoof and Hobbs [1].

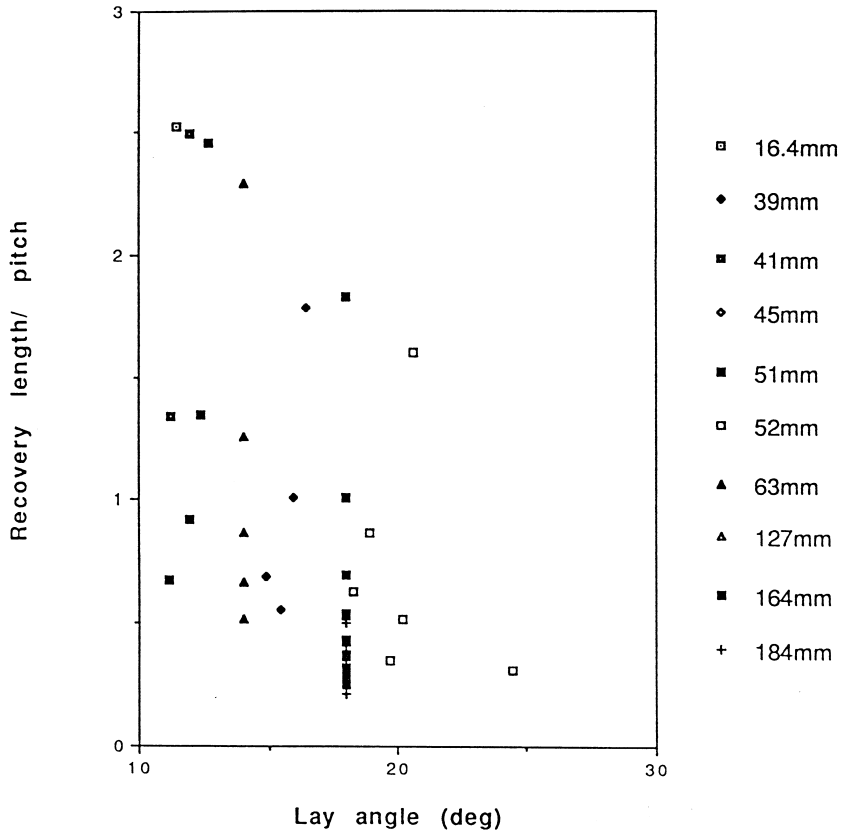

Fig. 4(a).

Very briefly, using Wyatt's [23] temperature measurements during axial cyclic tests (at 4.4 Hz) on 6 m-long 39 mm spiral strands, whose construction details are given elsewhere [8], the zone of end effects was found to extend about 2.6 lay lengths from either side: it may, then, be concluded that a specimen with $l/p = 5$ (where l = length of specimen; and p = lay length of the outer layer), will have virtually no central portion free from end effects. It should, however, be noted that those zones of end effects are only influenced by the disturbances to the lays of the cable during the terminating process by craftsmen, and should not be confused with the influence of recovery length of a fractured wire whose estimate is of relevance to the determination of only the desired minimum free-field length of the specimen, away from the terminations. As demonstrated in the previous section, an upper bound value of recovery length $l^{i}_{fs} = 2.5p$ may be assumed, irrespective of the associated lay angle and cable's degree of bedding-in (age), i.e. whether the pattern of normal (particularly line-contact) interwire forces have fully stabilised or not. As a pre-requisite to axial fatigue tests, therefore, a minimum free length in a test specimen of $l_c = 2\,l_{fs}$ or say five lay lengths seems essential. It then follows that, taken with the termination zone of influence (≈five lay lengths), the minimum desirable total length of test specimens should be around 10 lay lengths. Indeed, Chaplin [24] has (on the basis of experience) suggested the same figure as a minimum specimen length. Note that this minimum desirable length is applicable to both spiral strands and wire ropes of any construction.

As discussed previously, most codes of practice for rope inspection require rope replacement when a specified number of fractured wires are found to have occurred over a certain control length. For example, BS6570 [25] recommends a control length of 10 rope diameters (i.e. about 1.5 rope lay lengths), while the corresponding figures recommended by ISO4309 [26] are 6 rope diameters (about one rope lay length), and 30 rope diameters (about five rope lay lengths). The visible wire break discard criteria as specified by BS6570 [25] and ISO 4309 [26] primarily address the case of ropes bending over sheaves, and as discussed by Chaplin and Potts [27], the applicability of visible outer wire discard criteria for ropes subjected to axial

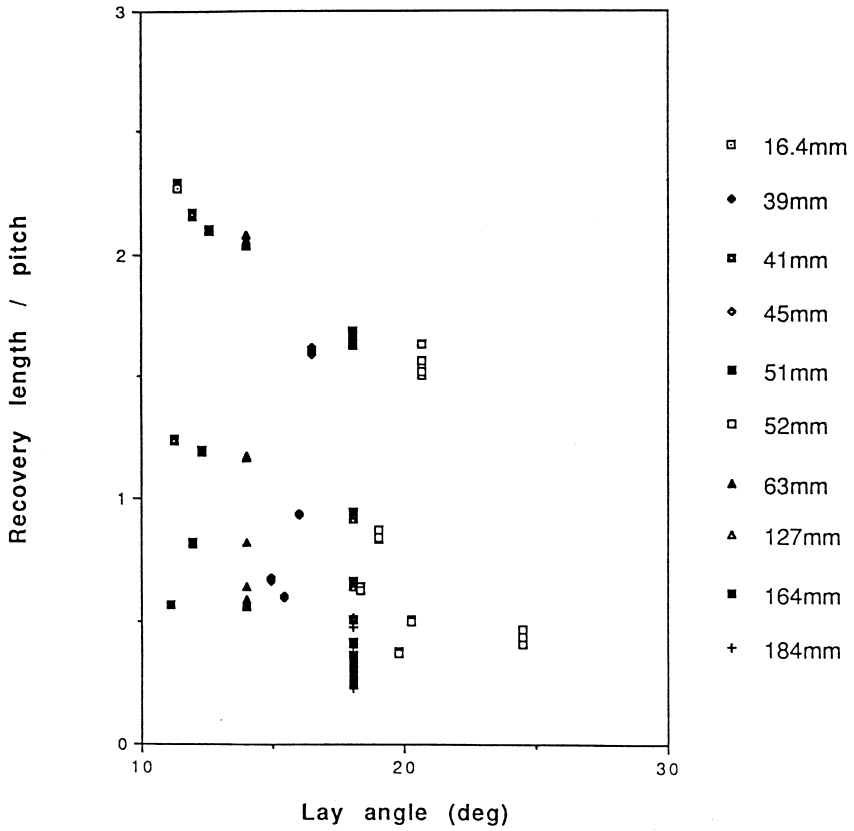

Fig. 4. Variations of recovery length with changes in the values of lay angle in various layers of a number of spiral strand constructions based on the assumption of zero line-contact interwire normal forces: (a) orthotropic sheet theory; (b) Leclair's theory.

loading and not passing over a pulley is dubious and previous experimental attempts have been inconclusive.

For the case of axial fatigue loading on multi-layered spiral strands, Raoof [28] has developed a theoretical model backed by an extensive series of large scale test data from different institutions on specimens from a number of different rope manufacturers [28–31]. The theoretical model is capable of predicting the number of axial fatigue cycles to first outer (or inner) wire fractures, and is applicable to any type of multi-layered spiral strand construction. According to Raoof's theoretical model, it is the magnitude of stress concentration factors over the trellis points of interlayer contact that control first wire fractures depending on the level of nominal axial stress in the wires. Based on his model, for a fractured wire to develop another fracture along its length under axial cyclic loading, the broken wire must develop its original level of mean axial stress which (as shown in the present paper) takes place along a distance equal to the associated recovery length: with the nominal wire axial stress reaching its full magnitude, the associated stress concentration factor over a trellis contact patch located at the end of recovery length will be high enough to theoretically cause another fracture along this same wire. It may, then, be reasonably concluded that the minimum spacing of potential fractures along a helical wire is *one* recovery length. In order words, for cable discard purposes based on the number of broken wires, a control length equal to one recovery length is essential. Noting that (as discussed previously) the fitted curve in Fig. 3(b) provides a reasonable upper bound estimate of recovery length in not only spiral strands but also wire ropes, this curve may also be utilised for determining the appropriate value of control length to be used for cable discard purposes. From Fig. 3(b) and 4, a control length of 2.5 lay lengths may reasonably be suggested for any type of steel cable (spiral strand and/or wire rope) construction, with any age (i.e. working life), subjected to axial fatigue loading.

6. Conclusions

The full set of formulations for determining the magnitude of recovery length in axially loaded spiral strands with special emphasis placed on the method(s) of solution for the final complex equation, are presented in some detail.

Solutions are provided for two extreme cases: in case [1], the presence of both hoop and radial normal interwire contact forces in fully bedded-in strands are catered for, while in case [2], the extreme condition is considered when (in the presence of gaps between the adjacent wires in a layer) no line-contact normal forces exist in the hoop direction with only the radial interwire contact forces being present.

Theoretical formulations using both the previously reported orthotropic sheet concept (with and/or without line-contact forces), and Leclair's method, which only caters for the presence of radial interwire contact forces, are reported.

Based on a series of previously reported theoretical parametric studies, simple recommendation are made for determining the control length for steel cables (spiral strands and/or wire ropes) along which the number of broken wires should be counted for cable discard purposes. It is argued that an upper bound value of 2.5 lay lengths (equal to the upper bound to the magnitude of one recovery length) may reasonably be used as a control length for both spiral strands and/or wire ropes with any type of construction.

The practical value of recovery length, (which primarily depends on the lay angle) in terms of determining the minimum length of test specimens for axial fatigue testing so that the so-obtained results may be used for estimating the axial fatigue lives of the much longer cables under service conditions, is also discussed. Using the data based on theoretical parametric studies, it is argued that a minimum specimen length of 10 lay lengths (irrespective of the type of cable construction) should ideally be used for axial fatigue tests.

Acknowledgements

The long standing and friendly co-operation of Bridon Ropes Personnel in Doncaster, UK, is gratefully acknowledged.

References

[1] Raoof M, Hobbs RE. Analysis of axial fatigue data for wire ropes. International Journal of Fatigue 1994;16:493–501.
[2] Davidsson W. Investigation and calculation of the remaining tensile strength in wire ropes with broken wires. ACTA Polytechnica, Mechanical Engineering Series, 1955;3.
[3] Wiek L, The influence of broken wires on wire rope strength and discarding. Organisation Internationale pour l'Etude de l'Endurance des Cables (OIPEEC), Round Table Conference, Luxembourg, October, 1977.
[4] Hankus J, Safety factor for hoisting rope weakened by fatigue cracks in wires. Organisation Internationale pour l'Etude de l'Endurance des Cables (OIPEEC), Round Table Conference, Krakow, June, 1981.
[5] Chaplin CR, Tantrum NRH, The influence of wire break distribution on strength. Organisation Internationale pour l'Etude de l'Endurance des Cables (OIPEEC), Round Table Conference, NEL Glasgow, June, 1985.

[6] Chein CH, Costello GA. Effective length of a fractured wire in wire rope. Journal of Engineering Mechanics, ASCE 1985;111(7):952–61.
[7] Raoof M. Wire recovery length in a helical strand under axial-fatigue loading. International Journal of Fatigue 1991;13(2):127–32.
[8] Raoof M, Hobbs RE. Analysis of multi-layered structural strands. Journal of Engineering Mechanics, ASCE 1988;114:1166–82.
[9] Raoof M, Hobbs RE. Tangential compliance of rough elastic bodies in contact. Journal of Tribology, ASME 1989;111:726–9.
[10] Raoof M, Huang YP. Wire recovery length in suspension bridge cable. Journal of Structural Engineering, ASCE 1992;118(12):3255–67.
[11] Gjelsvik A. Development length for single wire in suspension bridge cable. Journal of Structural Engineering, ASCE 1991;117(4):1189–200.
[12] Raoof M, Kraincanic I. Recovery length in multi-layered spiral strands. Journal of Engineering Mechanics, ASCE 1995;121(7):795–800.
[13] Raoof M, Kraincanic I. Recovery length in sheathed spiral strands in deep-water platform applications. International Journal of Fatigue 1993;15(6):485–92.
[14] Leclair RA. Axial response of multilayered strands with compliant layers. Journal of Engineering Mechanics, ASCE 1991;117(12):2884–903.
[15] Raoof M. Methods for analysing large spiral strands. Journal of Strain Analysis 1991;26(3):165–74.
[16] Phillips JW, Costello GA. Contact stresses in twisted wire cables. Journal of Engineering Mechanics Division, ASCE 1973;99(EM2):331–41.
[17] Costello GA, Phillips JW. A more exact theory for twisted wire cables. Journal of Engineering Mechanics Division, ASCE 1974;100(EM5):1096–8.
[18] Phillips JW, Miller RE, Costello GA. Contact stresses in a straight cross-lay wire rope. In: Proceedings of the First Annual Wire Rope Symposium, Denver, Colorado. Engineering Extension Service, Washington State University, Pullman, Washington, 1980:177–199.
[19] Hobbs RE, Raoof M. Interwire slippage and fatigue prediction in stranded cables for TLP tethers. In: Chryssostomidis C, Connor JJ, editors. Behaviour of offshore structures (Proceedings, 3rd International Conference on Behaviour of Offshore Structures, MIT, Cambridge, MA). Hemisphere Publishing/McGraw-Hill, New York, 1982;2:77–99.
[20] Shoup TE. Numerical methods for the personal computer. London: Prentice-Hall, 1983.
[21] Raoof M, Hobbs RE. Torsion tests on large spiral strands. Journal of Strain Analysis 1988;23(2):97–104.
[22] Raoof M. Comparison between the performance of newly manufactured and well-used spiral strands. Proceedings of the Institution of Civil Engineers, Part II. 1990;89:103–120.
[23] Wyatt TA. Internal Damping in 38 mm (nominal) specimens. Imperial College, Civil Engineering Department, CESLIC Report SC2, 1978.
[24] Chaplin CR. Tensile fatigue of very short samples of stranded wire rope. In: Proceedings of IABSE Workshop; Length Effect on Fatigue of Wires and Strands, Report 66. IABSE, Zürich, Switzerland, 1992;201–11.
[25] BS6570. Code of practice for the selection, care and maintenance of steel wire ropes. British Standards Institution, 1986.
[26] ISO4309. Cranes-wire ropes—code of practice for examination and discard. International Organisation for Standardisation, 1990.
[27] Chaplin CR, Potts AE. Wire rope offshore—a critical review of wire rope endurance research affecting offshore applications. University of Reading Research Report for Department of Energy, HMSO Publication OTH91341, 1991.
[28] Raoof M. Axial fatigue of multi-layered strands. Journal of Engineering Mechanics, ASCE 1990;116(10):2083–99.
[29] Raoof M. Axial fatigue life prediction of bridge cables. In: Harding JE, Parke GAR, Rayll MJ, editors. Proceedings of the Third International Conference on Bridge Management, Inspection, Assessment and Repair. E&FN Spon, University of Surrey, Guildford, Surrey, UK, 1996;523–31.
[30] Alani A, Raoof M. Axial fatigue characteristics of large diameter spiral strands. In Proceedings of 5th International Offshore and Polar Engineering Conference. Chung JS, *et al.* (Eds) Hague, The Netherlands. 1995;II: 260–265.
[31] Raoof M, Alani M. Axial fatigue of spiral strands in offshore platform applications. In: Chung JS, Frederking RMW, Saeki H, Bekker AT, editors. Proceedings of the 7th International Offshore and Polar Engineering Conference. Honolulu, Hawaii, USA, 1997;II:169–176.